

See discussions, stats, and author profiles for this publication at: <https://www.researchgate.net/publication/320992079>

"Natural convection flow in a solar dryer geometry"

Article · November 2017

CITATIONS

0

READS

29

2 authors, including:



Bernardo López-Sosa

Universidad Michoacana de San Nicolás de Hidalgo

12 PUBLICATIONS 15 CITATIONS

[SEE PROFILE](#)

Some of the authors of this publication are also working on these related projects:



Desarrollo de tecnologías sustentables [View project](#)



Ecotechnologies [View project](#)

Tema A4. Termofluidos: Energía

“Natural convection flow in a solar dryer geometry”

José Núñez^{a*}, Alberto Beltrán^b, Carlos A. García^a, Bernardo López-Sosa^c

^aEscuela Nacional de Estudios Superiores, Unidad Morelia, Universidad Nacional Autónoma de México, Antigua Carretera a Pátzcuaro No. 8701, Col. Ex Hacienda de San José de la Huerta, 58190, Morelia, Michoacán, México.

^bInstituto de Investigaciones en Materiales, Unidad Morelia, Universidad Nacional Autónoma de México, Antigua Carretera a Pátzcuaro No. 8701, Col. Ex Hacienda de San José de la Huerta, C.P. 58190, Morelia, Michoacán, México.

^cInstituto de Investigación en Metalurgia y Materiales, Universidad Michoacana de San Nicolás de Hidalgo, Gral. Francisco J. Mugica S/N, Ciudad Universitaria, 58030 Morelia, Mich.

*Autor contacto. joseng@enesmorelia.unam.mx

RESUMEN

En este trabajo se presenta un estudio numérico de la convección natural de aire en una geometría idealizada de un secador solar. Se impone una diferencia de temperatura entre las paredes inferior y superior de la cavidad mientras que las paredes laterales se consideran adiabáticas. Las ecuaciones gobernantes para la convección natural se resuelven numéricamente utilizando el software de modelado COMSOL Multiphysics®. Los patrones de flujo y las distribuciones de temperatura se obtienen para seis configuraciones diferentes y para cada una de ellas se evalúa el rendimiento de la transferencia de calor calculando el número de Nusselt en la pared inferior en función del número de Rayleigh. Los resultados indican que la transferencia de calor es mayor en una doble cavidad inclinada que en las otras configuraciones.

Palabras Clave: Convección Natural; Secador solar, Simulación numérica.

ABSTRACT

In this work, a two-dimensional numerical study of natural convection of air in an idealized solar dryer geometry is presented. A temperature difference is imposed between the bottom and top walls of the cavity while the sidewalls are considered insulated. The governing equations for natural convection are solved numerically using COMSOL Multiphysics® Modeling Software. The flow patterns and temperature distributions are obtained for six different geometries. The heat transfer performance is evaluated by calculating the Nusselt number on the bottom wall as a function of the Rayleigh number. Results show that heat transfer is higher in a double tilted cavity than in the other configurations.

Keywords: Natural convection; solar dryer geometry, numerical simulation.

1. Introduction

A literature review indicates the numerical study of heat transfer by natural convection in trapezoidal or triangular, shaped geometries has received a notable attention because of its importance in various engineering applications such as building and thermal insulation [1, 2], solar distillation [3] and solar heated, lumber dry kiln designs [4, 5]. Basically, two groups of solar energy dryers can be identified, passive or natural circulation and active or forced convection solar energy dryers, this last category is often called hybrid solar dryers [6].

Kamiyo et al. [2] performed a numerical study for the laminar air flow and temperature distributions in asymmetric rooftop-shaped triangular enclosures heated

isothermally from the base wall, for various aspect ratios, and Rayleigh number values. In the work from Omri et al. [3], they studied a two-dimensional incompressible fluid flow inside a triangular enclosure with isotherm upper walls and heated bottom. They also explored, the hydrodynamic and thermal fields, the local Nusselt number, the temperature profiles at the bottom and at the center of the cavity for a large range of Rayleigh numbers. In the same direction, Saha et al. [7] presented a numerical study of unsteady natural convection in an isosceles triangular enclosure subject to nonuniformly cooling at the inclined surfaces and uniformly heating at the base; the flow inside the enclosure depends significantly on the governing parameters such as Rayleigh number and aspect ratio.

Solar energy has been considered for lumber drying; for instance, Bentayeb et al. [8] presented a numerical simulation of a wood solar dryer under atmospheric conditions for the Moroccan climate. Martinez et al. [5] presented a simplified mathematical model to simulate the performance of a solar lumber dryer in Mexico; they carried out a comparison between experimental and theoretical results.

Further modeling and analysis are needed to estimate temperature variations, air flow and moisture removal rates that could lead to optimum parameters like: orientation, size, and operating conditions for a solar heated, lumber dry kiln. In this direction, the present study aims to examine through numerical simulations the influence of natural convection in a solar dryer.

In Section 2, the geometries under study are shown, as well as the governing equations, dimensionless parameters and boundary conditions. In Section 3, the numerical procedure is detailed explained. Section 4 shows the code validation with a benchmark test of natural convection; while in Section 5 the main results are shown. Finally, some concluding remarks are drawn in Section 6.

2. Problem formulation

The simplest geometry for a solar dryer lumber kiln might be a square room; however, to improve solar energy collection an inclined roof is desirable. Figure 1 shows three different idealized solar dryer configurations (SDC). For all geometries, the bottom wall is considered to be at a high temperature, T_H , whereas the top wall is at low temperature, T_C ($T_H > T_C$), the laterals walls are considered adiabatic.

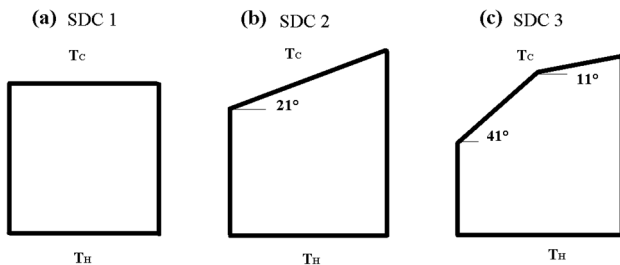


Figure 1 – Idealized geometries for a solar dryer.

Figure 1(a) corresponds to a square cavity heated from below and cooled from above, while Figure 1(b) represents a cavity with an inclined top wall; finally, Figure 1(c) shows a double inclined top wall cavity (angles are indicated in the figure).

The working fluid is assumed to be air; its physical properties are well known [9], the density, ρ , specific heat capacity, c_P , thermal conductivity, κ , thermal expansion coefficient, β , thermal diffusivity, α , and air kinematic viscosity, ν .

The flow inside the cavity is solved by using the governing equations for natural convection [10, 11], which are mass, momentum and energy conservation equations, with the Boussinesq approximation. The height of the cavity, L , the temperature difference, $\Delta T = T_H - T_C$, and the thermal diffusive velocity, $u_c = \alpha/L$, are used as characteristics scales.

The two-dimensional governing equations in dimensionless form are written as follows:

$$\frac{\partial u}{\partial x} + \frac{\partial v}{\partial y} = 0, \quad (1)$$

$$\frac{\partial u}{\partial t} + (\vec{u} \cdot \nabla)u = -\frac{\partial p}{\partial x} + \text{Pr} \nabla^2 u, \quad (2)$$

$$\frac{\partial v}{\partial t} + (\vec{u} \cdot \nabla)v = -\frac{\partial p}{\partial y} + \text{Pr} \nabla^2 v + \text{Ra Pr} T, \quad (3)$$

$$\frac{\partial T}{\partial t} + (\vec{u} \cdot \nabla)T = \nabla^2 T. \quad (4)$$

Where $x, y, t, \vec{u} = (u, v), p$ and T , are spatial dimensions, time, velocity, pressure and temperature fields, respectively. The differential operators are

$$\vec{u} \cdot \nabla = u \frac{\partial}{\partial x} + v \frac{\partial}{\partial y}, \quad (5)$$

$$\nabla^2 = \frac{\partial^2}{\partial x^2} + \frac{\partial^2}{\partial y^2}. \quad (6)$$

The boundary conditions for this problem are:

i) Constant temperature in the top and bottom walls

$$T=1 \text{ on bottom wall, } T=0 \text{ on top wall.} \quad (7)$$

ii) Thermal insulation in the laterals walls

$$\frac{\partial T}{\partial x} = 0 \text{ on left and right wall.} \quad (8)$$

iii) No-slip condition for the velocity at all walls

$$\vec{u} = 0, \quad (9)$$

iv) and finally, the initial condition is

$$T(x, y, t = 0) = 0.5. \quad (10)$$

As can be seen from Eqs. (1-6), the flow is characterized by two dimensionless parameters, the Rayleigh number, Ra, and the Prandtl number, Pr, which are defined as

$$Ra = \frac{g\beta(T_H - T_C)L^3}{\nu\alpha}, \quad Pr = \frac{\nu}{\alpha}, \quad (11)$$

where g is the gravity constant. Natural convection is governed by a dimensionless number called the Grashof number, which represents the ratio of the buoyancy force to the viscous force acting on the fluid and is expressed as

$$Gr = \frac{g\beta(T_H - T_C)L^3}{\nu^2} = \frac{Ra}{Pr} \quad (12)$$

To evaluate the heat transfer performance in all geometries, the local and average Nusselt number are used, and they are defined as

$$Nu_L = -\frac{\partial T}{\partial y} \Big|_{y=0}, \quad Nu_{av} = \int_0^1 Nu_L dx. \quad (13)$$

Both parameters are evaluated on the bottom (hot) wall.

3. Numerical methodology

Numerical solutions were obtained with COMSOL Multiphysics® Modeling Software 5.2a [12], which is a finite element analysis (FEA) simulation software for various physics and engineering applications.

Unstructured triangular meshes were implemented for all geometries. At least 2518 grid elements were used for the final simulations, after a series of grid testing. The use of body-fitted meshes having the corners inflated with nodes tightly clustered, is expected to guarantee good accuracy in the calculation of the local and mean Nusselt numbers. Steady state solutions for the temperature and the velocity were carried out.

3.1. Software validation

Numerical results obtained with the COMSOL Multiphysics® software were validated by reproducing the Vahl Davis benchmark test of natural convection for a differentially heated square cavity, filled with air

(Pr=0.71), and the Rayleigh number in the range of 10^3 to 10^6 [13].

Table 1 shows comparisons for the stream function at the midpoint of the cavity, $\psi^{mid}=\psi(0.5,0.5)$, the maximum horizontal velocity at the vertical midplane, u_{max} , the maximum vertical velocity at the horizontal midplane, v_{max} , and the average Nusselt number, Nu_{av0} , on the vertical hot wall ($x=0$).

Table 1 – Vahl Davis benchmark test.

Ra	ψ^{mid}	u_{max}	v_{max}	Nu_{av0}	Reference
10^3	1.174	3.649	3.697	1.118	Vahl Davis (1983)
	1.172	3.644	3.69	1.117	Present work
10^4	5.071	16.178	19.617	2.243	Vahl Davis (1983)
	5.075	16.178	19.632	2.242	Present work
10^5	9.111	34.73	68.59	4.519	Vahl Davis (1983)
	9.098	34.745	68.199	4.512	Present work
10^6	16.32	64.63	219.36	8.8	Vahl Davis (1983)
	16.381	64.869	218.03	8.82	Present work

Results given in Table 1 show that calculations reported in literature are reproduced with good agreement.

4. Results and discussions

4.1. Base configurations

Natural convection heated from below and cooled from above is also known as the Rayleigh-Benard problem. At low Ra numbers there is static balance since the temperature distribution depends only on the altitude, $T = T(y)$. Otherwise, when the vertical temperature gradient magnitude exceeds a certain value, given in terms of Ra number, convective motion occurs. This critical Rayleigh number can be determined using linear stability theory; in particular, the onset of natural convection takes place at $Ra > 1700$ [14].

The first configuration under study, SDC 1 (sketched in Figure 1(a)) is a square cavity heated from below and cooled from above. Temperature distributions at steady state from $Ra=10^3$ to $Ra=10^6$ are presented in Figure 2.

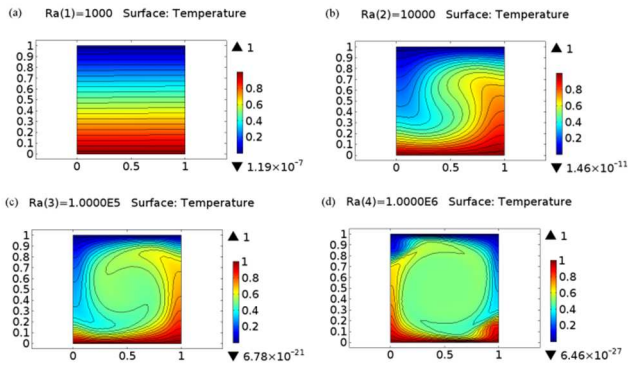


Figure 2 – SCD 1 temperature distributions
(a) $Ra=10^3$; (b) $Ra=10^4$; (c) $Ra=10^5$; (d) $Ra=10^6$.

The convective pattern consists of a single convective cell rotating clockwise with its center located at the geometric center of the cavity. Ascending and descending boundary layers near the walls are found in the lower left and upper right regions, respectively. At $Ra=10^6$, small vortex structures are observed in the left upper corner and right lower corner.

In Figure 3 the results for an inclined top wall geometry, SDC 2 are shown.

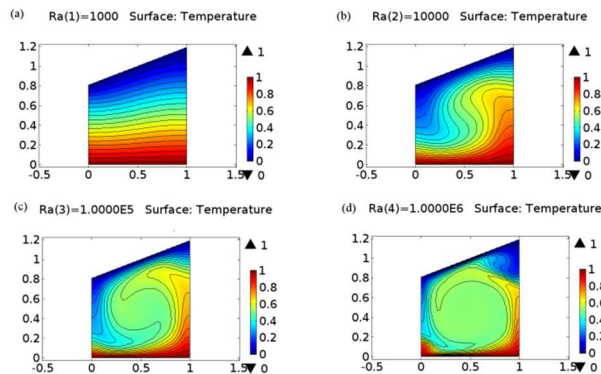


Figure 3 – SDC 2 temperature distributions.
(a) $Ra=10^3$; (b) $Ra=10^4$; (c) $Ra=10^5$; (d) $Ra=10^6$.

The vortex center is located slightly above the horizontal midplane of the cavity. At $Ra=10^6$, a single recirculation zone is observed in the right upper corner. It is also observed that a thermal plume emerging from bottom hits the top wall.

Figure 4 displays the temperature field for the SDC3 geometry.

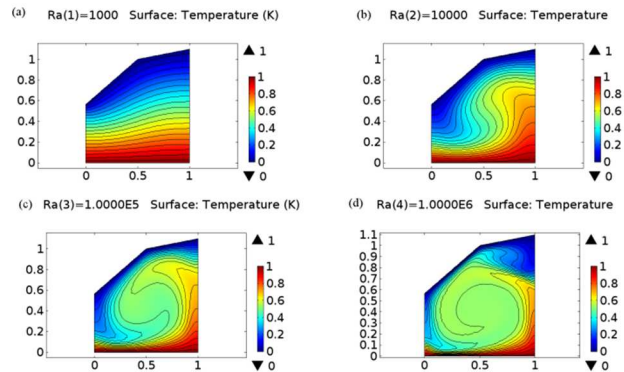


Figure 4 – SDC3 temperature distributions
(a) $Ra=10^3$; (b) $Ra=10^4$; (c) $Ra=10^5$; (d) $Ra=10^6$.

The observed convective pattern in these figures represents a deformed convective cell with a big vortex structure in the right upper and a small one in the right lower corner.

4.2. Effect of the aspect ratio

The aspect ratio is a dimensionless quantity usually defined as $A=Height/Width$, its effect on the flow and thermal behavior is now considered. In particular, similar geometrical configurations with an aspect ratio, $A=1/3$, are explored; see Figure 5.

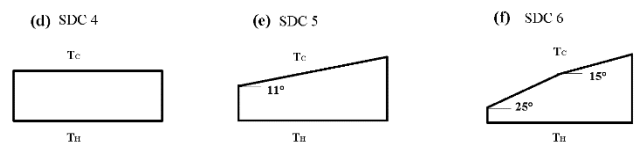


Figure 5 – Elongated idealized geometries for a solar dryer, $A=1/3$.

As can be seen for the SDC 4 geometry in Figure 6, horizontally elongated geometries typically introduce new instabilities, which break the basic roll into more than one. Now two or three convective cells take place in the system. In this configuration a small perturbation of order 10^{-3} was added for the volumetric force on the horizontal direction, to get a non-axisymmetric solution and in order to avoid a multiplicity solutions.

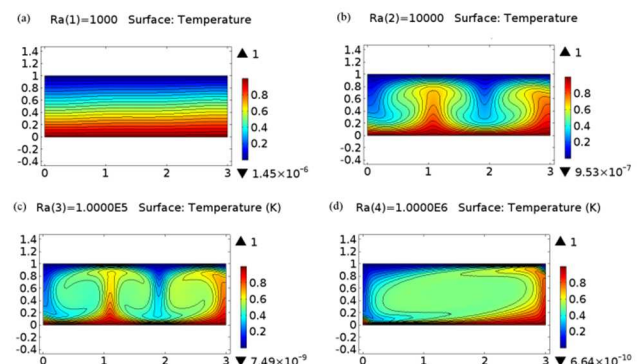


Figure 6 – SDC 4 temperature distributions
(a) $Ra=10^3$; (b) $Ra=10^4$; (c) $Ra=10^5$; (d) $Ra=10^6$.

On the other hand, for the geometrical configuration SDC 5, three convective cells are present for low Ra number

whereas two bigger cells appears for high Ra numbers, see Figure 7.

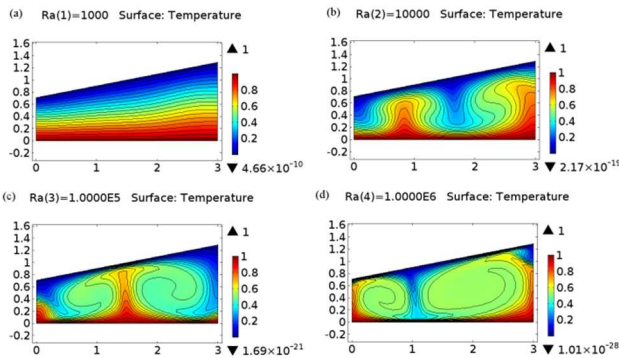


Figure 7 – SDC 5 temperature distributions

(a) $Ra=10^3$, (b) $Ra=10^4$, (c) $Ra=10^5$ and (d) $Ra=10^6$.

For the case of an elongated double tilted cavity, SDC 6, results also show that two or three convective cells appear as Ra increases, as can be seen in Figure 8.

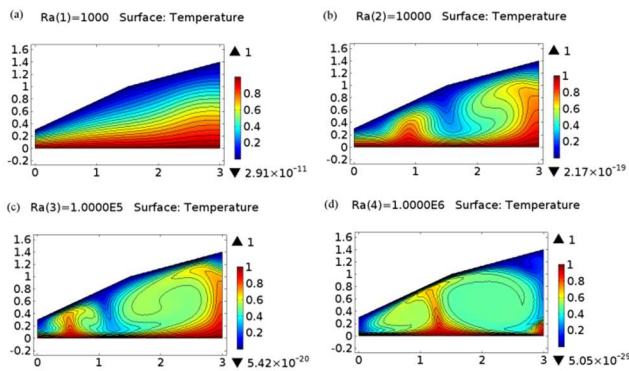


Figure 8 – SDC 6 temperature distributions

(a) $Ra=10^3$; (b) $Ra=10^4$; (c) $Ra=10^5$; (d) $Ra=10^6$.

4.3. Heat Transfer Behavior

The heat transferred throughout the bottom wall, can be described using the local Nusselt number, see Figure 9.

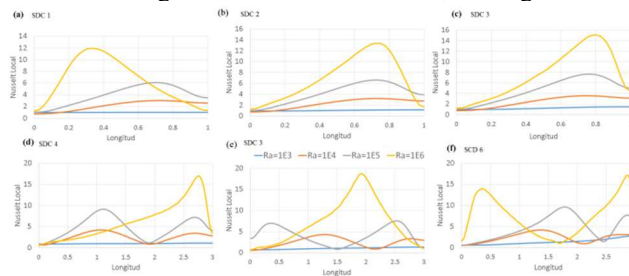


Figure 9 – Local Nusselt number on bottom wall for all configurations

$Ra=10^3$ (blue), $Ra=10^4$ (red), $Ra=10^5$ (gray), $Ra=10^6$ (orange).

In nearly square cavities, named SDC 1, SDC 2 and SDC 3, there is a main single vortex and for all of them, the local Nusselt number has a maximum value near the wall

where the hot fluid ascends. For small aspect ratio cavities, SDC 4, SDC 5 and SDC 6, multiple vortices appears and a second local maximum value occurs in the local Nusselt number, depending of the Rayleigh number.

The correlations for the Nusselt number $Nu = hL/k$ in natural convection are expressed in terms of the Rayleigh number; in Figure 10 the variation of the average Nusselt number as function of Ra for all geometries is shown. It is clear that the mean Nusselt number increases, as long as Ra increases.

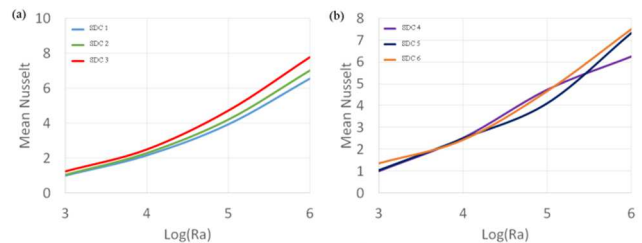


Figure 10 – Global Nusselt number vs. Rayleigh number

(a) SDC 1, SDC 2 and SDC 3; (b) SDC 4, SDC 5 and SDC 6.

It should be noticed that the values for Nusselt number in geometrical configuration SDC 3 (which corresponds to a double tilted cavity) is greater than in the other configurations, this might be explained due to the increment of the top cooled area.

5. Conclusions

Comprehensive simulations results on the natural convection in up to six configurations for an idealized solar dryer geometries were conducted using COMSOL Multiphysics® Modeling. For nearly square cavities a big convective cell is observed, while the Nusselt number shows a single maximum value. The effect of the aspect ratio was also studied and it was found that for the considered aspect ratio, two or three convective cells can occur; additionally, the Nusselt number exhibits more than one maximum values; therefore, zones with heat transfer enhancement can be determined.

All numerical simulations were performed under the two dimensional assumption, which, of course, is only partially representative of the real physics within the system. In the future, the study can be extended to include three dimensional effects on laminar flow and heat transfer, also different thermal boundary conditions such as constant heat flux or radiation and unsteady flow; finally, a deeper analysis of heat transfer under turbulent conditions would be important for more real-world applications.

Acknowledgments

Authors thank UNAM-DGAPA-PAPIIT for support under Project TA101117 and SENER-CONACyT Project 246911.

REFERENCES

- [1] O. M. Kamiyo, D. Angeli, G. S. Barozzi, M. W. Collins, V.O.S. Olunloyo, and S.O. Talabi. A comprehensive review of natural convection in triangular enclosures. *Applied Mechanics Reviews*, **63**, (2010).
- [2] O. M. Kamiyo, D. Angeli, G. S. Barozzi, and M. W. Collins. Natural convection in asymmetric triangular enclosures heated from below. *Journal of Physics: Conference Series*, **547**, (2014).
- [3] A. Omri, J. Orfi, and S. B. Nasrallah. Natural convection effects in solar stills. *Desalination*, **183**, (2005).
- [4] K. J. Taylor and A. D. Weir. Simulation of a solar timber drier. *Solar Energy*, **34**, (1985).
- [5] R. Martinez, E. Martinez, and F. Paez. Study of a solar lumber dryer in Mexico. *Solar and Wind Technology*, **1**, (1984).
- [6] S. C. Saha and Y. T. Gu. Natural convection in a triangular enclosure heated from below and non-uniformly cooled from top. *International Journal of Heat and Mass Transfer*, **80**, (2015).
- [7] F. Bentayeb, N. Bekkioui, and B. Zeghmati. Modelling and simulation of a wood solar dryer in a Moroccan climate. *Renewable Energy*, **33**, (2008).
- [8] O.V. Ekechukwu and B. Norton. Review of solar-energy drying systems II: an overview of solar drying technology. *Energy Conversion and Management*, **40**, (1999).
- [9] J. Núñez, M. Lopez-Caballero, E. Ramos, G. Hernandez-Cruz, M. Vargas, and S. Cuevas. Verification and experimental validation of a numerical simulation of natural convection in a slender cylinder. *International Journal of Heat and Fluid Flow*, **38**, (2012).
- [10] J. Núñez, E. Ramos, and J. M. Lopez. A mixed Fourier–Galerkin–finite-volume method to solve the fluid dynamics equations in cylindrical geometries. *Fluid Dynamics Research*, **44**, (2012).
- [11] Y. A. Cengel and M. A. Boles. *Termodinámica*. Mc Graw Hill, (2009).
- [12] Comsol. www.comsol.com. Accessed: 2017-04-05.
- [13] G. De Vahl Davis. Natural convection of air in a square cavity: A bench mark numerical solution. *International Journal for Numerical Methods in Fluids*, **3**, (1983).
- [14] J. C. Buell and I. Catton. The effect of wall conduction on the stability of a fluid in a right circular cylinder heated from below. *Journal of Heat Transfer*, **105**, (1983).